Inorganic Chemistry

Article

pubs.acs.org/IC

Differences in Nuclearity, Molecular Shapes, and Coordination Modes of Azide in the Complexes of Cd(II) and Hg(II) with a "Metalloligand" [CuL] (H_2L = *N*,*N*′-Bis(salicylidene)-1,3-propanediamine): Characterization in Solid and in Solutions, and Theoretical Calculations

Lakshmi Kanta Das,[†] Ramakant M. Kadam,[‡] Antonio Bauzá,[§] Antonio Frontera,*[,§] and Ashutosh Ghosh*[,†]

[†]Department of Chemistry, University College of Science, University of Calcutta, 92, A.P.C. Road, Kolkata-700 009, India

[‡]Radiochemistry Division, Bhabha Atomic Research Centre, Trombay, Mumbai 400085, India

[§]Department of Chemistry, Universitat de les Illes Balears, Crta de Valldemossa km 7.5, 07122 Palma de Mallorca, Baleares, Spain

Supporting Information

ABSTRACT: Two new heterometallic copper(II)−mercury(II) complexes $[(CuL)Hg(N_3)_2]_n$ (**1**) and $[(CuL)_2Hg(N_3)_2]$ (**2**) and one copper(II)−cadmium(II) complex $[(CuL)_2Cd(N_3)_2]$ (**3**) have been synthesized using "metalloligand" [CuL] (where H_2L = *N*,*N*′-bis(salicylidene)-1,3-propanediamine) and structurally characterized. Complex **1** is a one-dimensional (1D) helical coordination polymer constructed by the joining of the dinuclear $[(CuL)Hg(N_3)_2]$ units through a single $\mu_{-1,1}$ azido bridge. In the dinuclear unit the Hg(II) is bonded with two phenoxido oxygen atoms of "metalloligand" [CuL] and two nitrogen atoms of azido ligands. Complex **2** is a linear trinuclear entity, in which two terminal "metalloligands" [CuL] are coordinated to central Hg(II) through double phenoxido bridges. The azido ligands link the central mercury atom with the terminal copper atoms *via* $\mu_{-1,3}$ bridges. In contrast, the trinuclear complex **3** is bent. Here, in addition to two double phenoxido bridges, central Cd(II) is bonded to two mutually *cis* nitrogen atoms of two terminal azido ligands. The variation in the coordination modes of the azido ligand seems to be responsible for the different molecular shapes of **2** and **3**. Interestingly, bond distances between the Hg atoms and the central nitrogen atom of the azido ligands are 2.790(4) and 2.816(5) Å in **1** and 2.823(4) Å in **2**. These bond distances are significantly less than the sum of van der Waals radii of mercury (2.04 Å) and nitrogen (1.55 Å) and considerably longer than the sum of their covalent radii (2.03 Å). However the distances are similar to reported Hg−N bond distances of some Hg(II) complexes. Therefore, we have performed a theoretical density functional theory study to know whether there is any interaction between the central nitrogen atom of the azido ligand and the mercury atoms. We have used the Bader's "atoms-in-molecules", energetic and orbital analyses to conclude that such interaction does not exist. The probable reason for different molecular shapes observed in trinuclear complexes of **2** and **3** also has been studied and explained by theoretical calculations and using the CSD. Electronic spectra, EPR spectra and ESI mass spectra show that all three complexes lose their solid state identity in solution.

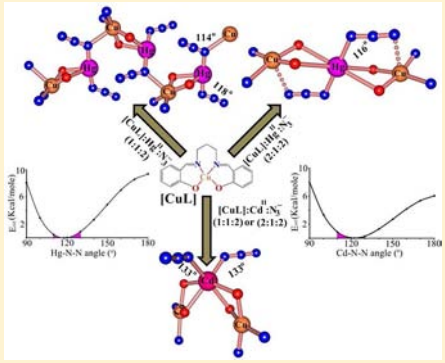

INTRODUCTION

In recent decades, the design and synthesis of heterometallic coordination complexes have attracted much attention of the chemists. The introduction of a heterometal center into the complexes may change the topologies[1,2] or may create unusual metal coordination environments that influence the physical properties of the materials, especially their catalytic, photoluminescent, and magnetic properties.[3−5] One of the common approaches for the synthesis of heterometallic complexes is to use a mononuclear complex of a divalent metal ion with salen type N_2O_2 donor ligand.[6−10] Usually, the oxygen atoms of one or two "metalloligands" coordinate to another metal ion along with the counteranions to result in dinuclear or trinuclear heterometallic complexes[11] respectively. It is important to mention that in most of the cases, the bridging bidentate anions (e.g., carboxylate, nitrate) result in linear trinuclear complexes,[12−15] whereas the monodentate anions (e.g., chloride, thiocyanate) form bent trinuclear complexes.[16−18] The azido ligand is well-known for its versatile bridging modes besides its monodentate terminal coordination.[19] Commonly, it binds the metal ions either through $\mu_{-1,1}$-N_3 or $\mu_{-1,3}$-N_3 bridging modes.[20−26] Other possible bridging modes of azido ligand are $\mu_{-1,1,1}$-N_3 and $\mu_{-1,1,3}$-N_3.[27] The rare variety of coordination

Received: August 13, 2012
Published: November 6, 2012

modes, e.g., $\mu_{-1,1,1,1}$-N_3, $\mu_{-1,1,3,3}$-N_3 and $\mu_{-1,1,1,3,3,3}$-N_3 have also been reported in some compounds.[28−30] It is to be noted that in all these cases, only the two terminal nitrogen atoms of the azido ligand are involved for bonding purposes.

As a part of our ongoing study in the development of heterometallic complexes,[31,32] we report here the synthesis, crystal structures, spectral properties and density functional theory (DFT) calculations of three new heterometallic complexes of Cd(II) and Hg(II) with "metalloligand" [CuL] [where H_2L = *N*,*N*′-bis(salicylidene)-1,3-propanediamine] and azide as coligand. Complex $[(CuL)Hg(N_3)_2]_n$ (**1**) is a one-dimensional (1D) helical coordination polymer, $[(CuL)_2Hg(N_3)_2]$ (**2**) is a linear trinuclear entity, whereas $[(CuL)_2Cd(N_3)_2]$ (**3**) is a bent trinuclear species. Interestingly, the distances between the Hg atoms and the central nitrogen atom of the azido ligand in **1** and **2** are rather short. In the literature, such short distances are reported but whether they should be considered as a bond between the two is an unexplored point that deserves further analysis. The reported structures exhibit Hg−N distances that lie between the sum of the covalent radii (2.03 Å) and the sum of their van der Waals radii (3.59 Å) of mercury and nitrogen.[33−39] Therefore, we have performed the theoretical study of both DFT and *ab initio* methods to analyze this aspect. We have used Bader's theory of "atoms-in-molecules" (AIM)[40] by the distribution of critical points to understand whether there is any interaction between the Hg atoms and the central nitrogen atom of the azido ligand, together with some energetic and orbital considerations to shed light on this issue. In addition, the discrete trinuclear complex **3** is significantly different from **2** since the two azido ligands are *cis* and consequently are not able to link the central cadmium atom with the terminal copper atoms *via* $\mu_{-1,3}$ bridges in **3**. Combining theoretical calculations and the analysis of the Cambridge Structural Database we provide a likely explanation for the different molecular shapes adopted by these two complexes.

EXPERIMENTAL SECTION

Starting Materials. The salicylaldehyde and 1,3-propanediamine were purchased from Lancaster and were of reagent grade. They were used without further purification.

Caution! Azide salt of metal complexes with organic ligands is potentially explosive. Only a small amount of material should be prepared and it should be handled with care.

Synthesis of the Schiff Base Ligand (H_2L) and the "Metalloligand" [CuL]. The Schiff base ligand was synthesized by a standard method. Briefly, 5 mmol of 1,3-propanediamine (0.42 mL) was mixed with 10 mmol of the salicylaldehyde (1.04 mL) in methanol. The resulting solution was refluxed for ca. 2 h and allowed to cool. The yellow colored methanolic solution was used directly for complex formation. To a methanolic solution (20 mL) of $Cu(ClO_4)_2·6H_2O$ (1.852 g, 5 mmol) was added a methanolic solution of H_2L (5 mmol, 10 mL) to prepare the "metalloligand" [CuL] as reported earlier.[41]

Synthesis of the Complex $[(CuL)Hg(N_3)_2]_n$ (1). The precursor "metalloligand" [CuL] (0.359 g, 1 mmol) was dissolved in methanol (20 mL) and then a water solution (1 mL) of $Hg(NO_3)_2·H_2O$ (0.342 g, 1 mmol) followed by an aqueous solution (1 mL) of sodium azide (0.130 g, 2 mmol) were added to this solution. A small amount of green precipitate separated immediately. The stirring was continued for 1 h at room temperature when the amount of the green solid increased. The solid was filtered and the filtrate was allowed to stand overnight in an open atmosphere when a needle shaped green (**1**) X-ray quality single crystals appeared at the bottom of the vessel. The crystals were washed with a methanol−water mixture and dried in a desiccator containing anhydrous $CaCl_2$ and then characterized by elemental analysis, spectroscopic methods, and X-ray diffraction.

Complex **1**: Yield: 0.514 g, 82% (with respect to both green precipitate and crystalline compound), Anal. Calc. for $C_{17}H_{16}HgCuN_8O_2$: C 32.49, H 2.57, N 17.83. found: C 32.58, H 2.52, N 17.71%. UV/vis: λ_{max} (MeOH) = 596, 359, and 269 nm, λ_{max} (DMSO) = 596, 361, and 274 nm and λ_{max} (solid, reflectance) = 615 and 387 nm. IR (KBr): ν(C═N) 1617 cm^{-1}, $\nu(N_3)$ 2045 cm^{-1}, HRMS (*m*/*z*, ESI^+): found for $[(CuL)H]^+$ = 343.95 (calc. 344.07), $[(CuL)Na]^+$ = 365.91 (calc. 366.05), $[(CuL)_2H]^+$ = 686.87 (calc. 687.13), $[(CuL)_2Na]^+$ = 708.80 (calc. 709.11), $[(CuL)_3Na]^+$ = 1053.78 (calc. 1054.16).

Synthesis of the Complex $[(CuL)_2Hg(N_3)_2]$ (2). Complex **2** was prepared by mixing the same components as for **1** but with different stoichiometric ratios. Briefly, the precursor "metalloligand" [CuL] (0.718 g, 2 mmol) was dissolved in methanol (20 mL), and then a water solution (1 mL) of $Hg(NO_3)_2·H_2O$ (0.342 g, 1 mmol) followed by an aqueous solution (1 mL) of sodium azide (0.130 g, 2 mmol) was added to this solution. As for compound **1**, here also a small amount of solid separated immediately but the color of the product was greenish brown. The stirring was continued for 1 h and then the solid was separated by filtration. The rectangular shaped greenish brown (**2**) X-ray quality single crystals were obtained by the slow evaporation of filtrate.

Complex **2**: Yield: 0.834 g, 86% (with respect to both greenish brown precipitate and crystalline compound), Anal. Calc. for $C_{34}H_{32}HgCu_2N_{10}O_4$: C 42.00, H 3.32, N 14.40. found: C 41.99, H 3.39, N 14.36%. UV/vis: λ_{max} (MeOH) = 596, 360, and 273 nm, λ_{max} (DMSO) = 597, 360, and 272 nm and λ_{max} (solid, reflectance) = 593 and 375 nm. IR (KBr): ν(C═N) 1614 cm^{-1}, $\nu(N_3)$ 2036 cm^{-1}, HRMS (*m*/*z*, ESI^+): found for $[(CuL)H]^+$ = 343.97 (calc. 344.07), $[(CuL)Na]^+$ = 365.94 (calc. 366.05), $[(CuL)_2H]^+$ = 686.91 (calc. 687.13), $[(CuL)_2Na]^+$ = 708.81 (calc. 709.11), $[(CuL)_3Na]^+$ = 1053.84 (calc. 1054.16).

Synthesis of the Complex $[(CuL)_2Cd(N_3)_2]$ (3). Complex **3** was prepared by mixing the same components and stoichiometric ratios as for **2** but using $Cd(NO_3)_2·4H_2O$ (0.309 g, 1 mmol) instead of $Hg(NO_3)_2·H_2O$. In this case, a small amount of brown product separated immediately, and it also increases gradually during stirring the mixture. The microcrystalline solid was separated by filtration. The filtrate on slow evaporation at room temperature yielded rectangular shaped brown X-ray quality single crystals.

Complex **3**: Yield: 0.736 g, 83% (with respect to both brown precipitate and crystalline compound), Anal. Calc. for $C_{34}H_{32}CdCu_2N_{10}O_4$: C 46.19, H 3.65, N 15.84 found: C 46.19, H 3.67, N 15.80%. UV/vis: λ_{max} (MeOH) = 601, 358, and 273 nm, λ_{max} (DMSO) = 597, 361, and 269 nm and λ_{max} (solid, reflectance) = 578 and 370 nm. IR (KBr): ν(C═N) 1614 cm^{-1}, $\nu(N_3)$ 2040 cm^{-1}, HRMS (*m*/*z*, ESI^+): found for $[(CuL)H]^+$ = 343.98 (calc. 344.07), $[(CuL)Na]^+$ = 365.95 (calc. 366.05), $[(CuL)_2H]^+$ = 686.92 (calc. 687.13), $[(CuL)_2Na]^+$ = 708.84 (calc. 709.11), $[(CuL)_3Na]^+$ = 1053.84 (calc. 1054.16).

Physical Measurements. Elemental analyses (C, H and N) were performed using a Perkin-Elmer 2400 series II CHN analyzer. IR spectra in KBr pellets (4000−500 cm^{-1}) were recorded using a Perkin-Elmer RXI FT-IR spectrophotometer. Electronic spectra in methanol as well as in DMSO and in solid state (750−300 nm) were recorded in a Hitachi U-3501 spectrophotometer. Powder X-ray diffraction patterns are recorded on a Bruker D-8 advance diffractometer operated at 40 kV voltage and 40 mA current and calibrated with a standard silicon sample, using Ni-filtered Cu-Ka (a = 0.15406 nm) radiation. EPR experiments were conducted using a BRUKER ESP-300 spectrometer operated at X-band frequency (9−10 GHz) with 100 kHz frequency modulation. DPPH was used as a reference material for calibration of g values. Temperature was varied in the range 100−300 K using variable temperature accessory Eurotherm BVT 2000 with liquid nitrogen as coolant in a flow system. The electrospray ionization mass spectrometry (ESI-MS positive) spectra were recorded with a Micromass Qtof YA 263 mass spectrometer.

Crystallographic Data Collection and Refinement. Suitable single crystals of each complex were mounted on a Bruker-AXS SMART APEX II diffractometer equipped with a graphite mono-

Table 1. Crystal Data and Structure Refinement of Complexes 1−3

complexes	1	2	3
formula	$C_{17}H_{16}HgCuN_8O_2$	$C_{34}H_{32}HgCu_2N_{10}O_4$	$C_{34}H_{32}CdCu_2N_{10}O_4$
M	628.52	972.39	884.21
crystal system	monoclinic	triclinic	triclinic
space group	$P2_1/c$	$P\bar{1}$	$P\bar{1}$
a/Å	14.1481(6)	9.488(5)	9.9049(9)
b/Å	14.8246(6)	9.937(5)	11.9411(11)
c/Å	9.8662(4)	10.299(5)	14.1966(14)
α/°	90	84.893(5	91.463(1)
β/°	108.243(1)	65.495(5)	101.660(1)
γ/°	90	76.198(5)	90.685(1)
V/Å^3	1965.33(14)	858.0(8)	1643.7(3)
Z	4	1	2
D_c/g cm^{-3}	2.124	1.882	1.786
μ/mm^{-1}	8.916	5.746	1.981
F(000)	1196	476	888
R(int)	0.041	0.031	0.026
total reflections	26710	11421	12049
unique reflections	5487	4834	5974
$I > 2\sigma(I)$	4269	3793	4481
R_1, wR_2	0.0333, 0.0851	0.0383, 0.1154	0.0384, 0.0977
temp (K)	293	293	293
GOF value	0.99	1.04	1.06

Table 2. Bond Distances (Å) and Angles (°) around Metal Atoms for Complexes 1 and 2[a]

complex 1		complex 2	
Hg(1)−O(1)	2.589(3)	Hg(1)−O(1)	2.762(4)
Hg(1)−O(2)	2.530(3)	Hg(1)−O(2)	2.687(4)
Hg(1)−N(11)	2.069(3)	Hg(1)−N(11)	2.079(6)
Hg(1)−N(21)	2.050(5)	Hg(1)−N(12)	2.823(4)
Hg(1)−N(12)	2.790(4)		
Hg(1)−N(22)	2.816(5)		
Cu(1)−O(1)	1.932(3)	Cu(1)−O(1)	1.923(4)
Cu(1)−O(2)	1.923(3)	Cu(1)−O(2)	1.920(4)
Cu(1)−N(1)	1.974(4)	Cu(1)−N(1)	1.978(5)
Cu(1)−N(2)	1.985(4)	Cu(1)−N(2)	1.981(5)
Cu(1)−N(11)[a]	2.630(4)	Cu(1)−N(13)	2.855(6)
O(1)−Hg(1)−O(2)	58.85(9)	O(1)−Hg(1)−O(2)	54.69(10)
O(1)−Hg(1)−N(11)	89.41(12)	O(1)−Hg(1)−N(11)	87.63(17)
O(1)−Hg(1)−N(21)	97.42(15)	O(2)−Hg(1)−N(11)	89.57(17)
O(2)−Hg(1)−N(11)	97.84(13)		
O(2)−Hg(1)−N(21)	85.90(15)		
N(11)−Hg(1)−N(21)	173.17(17)		
O(1)−Cu(1)−O(2)	81.45(12)	O(1)−Cu(1)−O(2)	81.32(15)
O(1)−Cu(1)−N(1)	91.83(15)	O(1)−Cu(1)−N(1)	92.50(17)
O(1)−Cu(1)−N(2)	162.63(14)	O(1)−Cu(1)−N(2)	169.1(2)
O(1)−Cu(1)−N(11)[a]	106.39(12)	O(1)−Cu(1)−N(13)	82.22(16)
O(2)−Cu(1)−N(1)	171.29(16)	O(2)−Cu(1)−N(1)	170.59(18)
O(2)−Cu(1)−N(2)	91.49(14)	O(2)−Cu(1)−N(2)	90.75(18)
O(2)−Cu(1)−N(11)[a]	81.59(12)	O(2)−Cu(1)−N(13)	98.72(17)
N(1)−Cu(1)−N(2)	96.47(17)	N(1)−Cu(1)−N(2)	96.3(2)
N(1)−Cu(1)−N(11)[a]	95.10(14)	N(1)−Cu(1)−N(13)	87.39(18)
N(2)−Cu(1)−N(11)[a]	88.10(13)	N(2)−Cu(1)−N(13)	91.62(19)

[a]Symmetry element: a = (x, 1/2 − y, −1/2 + z) for complex **1** and (2 − x, −y, 1 − z) for complex **2**.

chromator and Mo−Kα (λ = 0.71073 Å) radiation. The crystals were positioned at 60 mm from the CCD. Frames (360) were measured with a counting time of 5 s. The structures were solved using the Patterson method by using the SHELXS 97 program. The non-hydrogen atoms were refined with anisotropic thermal parameters. The hydrogen atoms bonded to carbon were included in geometric positions and given thermal parameters equivalent to 1.2 times those of the atom to which they were attached. Some disorder was apparent with the carbon atoms of the propylene link in the ligand of **1** and **2**. It was set up with C8a C9a C10a and C8b C9b C10b as separate parts

dx.doi.org/10.1021/ic301773h | Inorg. Chem. 2012, 51, 12407−12418

Table 3. Bond Distances (Å) and Angles (°) around Metal Atoms for Complex 3

Complex 3					
Cd(1)−O(1)	2.365(3)	O(1)−Cd(1)−O(2)	64.07(10)	O(1)−Cu(1)−O(2)	82.05(13)
Cd(1)−O(2)	2.372(3)	O(1)−Cd(1)−O(3)	99.31(11)	O(1)−Cu(1)−N(1)	90.93(15)
Cd(1)−O(3)	2.377(3)	O(1)−Cd(1)−O(4)	158.23(11)	O(1)−Cu(1)−N(2)	166.38(15)
Cd(1)−O(4)	2.343(3)	O(1)−Cd(1)−N(11)	101.70(14)	O(2)−Cu(1)−N(1)	164.91(17)
Cd(1)−N(11)	2.194(5)	O(1)−Cd(1)−N(21)	95.25(16)	O(2)−Cu(1)−N(2)	92.63(15)
Cd(1)−N(21)	2.214(4)	O(2)−Cd(1)−O(3)	75.56(11)	N(1)−Cu(1)−N(2)	97.00(17)
Cu(1)−O(1)	1.921(3)	O(2)−Cd(1)−O(4)	97.82(10)	O(3)−Cu(2)−O(4)	79.10(13)
Cu(1)−O(2)	1.907(3)	O(2)−Cd(1)−N(11)	96.64(15)	O(3)−Cu(2)−N(3)	91.75(15)
Cu(1)−N(1)	1.959(4)	O(2)−Cd(1)−N(21)	157.11(16)	O(3)−Cu(2)−N(4)	170.28(15)
Cu(1)−N(2)	1.944(4)	O(3)−Cd(1)−O(4)	62.78(11)	O(4)−Cu(2)−N(3)	170.29(15)
Cu(2)−O(3)	1.940(3)	O(3)−Cd(1)−N(11)	151.50(14)	O(4)−Cu(2)−N(4)	91.81(15)
Cu(2)−O(4)	1.921(3)	O(3)−Cd(1)−N(21)	99.81(14)	N(3)−Cu(2)−N(4)	97.51(17)
Cu(2)−N(3)	1.960(4)	O(4)−Cd(1)−N(11)	91.94(14)		
Cu(2)−N(4)	1.971(4)	O(4)−Cd(1)−N(21)	99.81(16)		
		N(11)−Cd(1)−N(21)	97.23(18)		

Scheme 1. Formation of Complexes 1−3

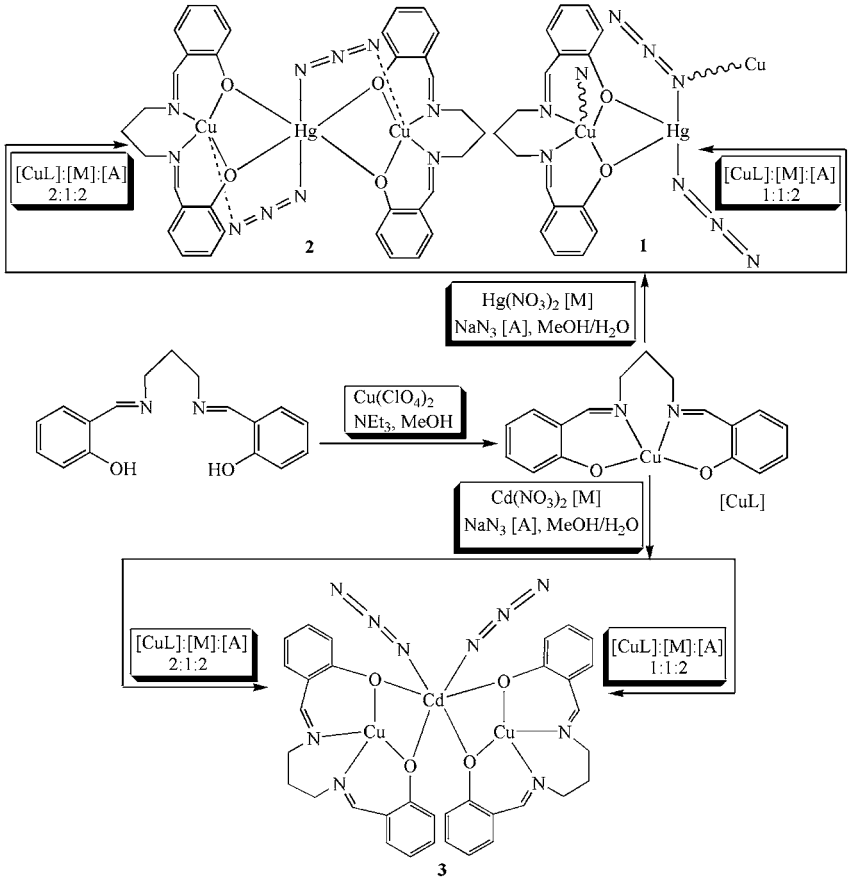

although C8a C8b and C10a C10b have the same coordinates and these positions were refined with occupation factors close to 50%. Successful convergence was indicated by the maximum shift/error of 0.001 for the last cycle of the least-squares refinement. Absorption corrections were carried out using the SADABS program.[42] All the calculations were carried out using SHELXS 97,[43] SHELXL 97,[44] PLATON 99,[45] ORTEP-32[46] and WINGX system ver-1.64.[47] Data collection, structure refinement parameters and crystallographic data for the three complexes are given in Table 1. The selected bond lengths and bond angles are summarized in Tables 2 and 3.

Theoretical Methods. All calculations were carried out using the Turbomole package version 6.10.[48] For the small model complexes we have used the RI-MP2 method and aug-cc-pVDZ basis set,[49] which has been widely used to study noncovalent interactions. The optimization has been performed without imposing symmetry constraints. The RI-MP2 method applied to the study of weak interactions is considerably faster than the MP2, and the interaction energies and equilibrium distances are almost identical for both methods.[50,51] We have recently demonstrated that this level of theory gives comparable results to the CCSD(T)/AVTZ//RI-MP2/aug-cc-pVQZ level for some weak interactions.[52] Because of the size of the system, for the calculations of compounds **1**−**3** we have used the crystallographic coordinates and the B87-D method, which includes the density functional correction for dispersion.[53] This level of theory is a good compromise between the size of the system and the accuracy of the results. To analyze the intramolecular interactions, the AIM theory was employed.[54] AIM is

dx.doi.org/10.1021/ic301773h | Inorg. Chem. 2012, 51, 12407−12418

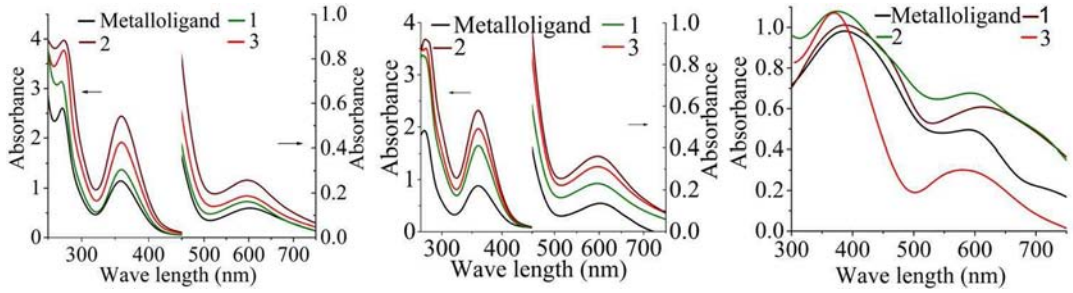

Figure 1. Electronic spectra of the complexes. Left: in MeOH, Middle: in DMSO and Right: in solid state.

based upon those critical points where the gradient of the density, $\nabla\rho$, vanishes. Such points are classified by the curvature of the electron density; for example, a bond critical point (CP) has one positive curvature (in the internuclear direction) and two negative ones (perpendicular to the bond). Two bonded atoms are then connected with a bond path through the bond CP. The properties evaluated at such bond CPs characterize the bonding interactions. They have been widely used to study a great variety of molecular interactions.[55−57]

RESULTS AND DISCUSSION

Synthesis of the Complexes. The Schiff-base ligand (H_2L) and its Cu(II) complex [CuL] were synthesized using the reported procedure.[41] The "metalloligand" [CuL] on reaction with mercuric nitrate monohydrate and the sodium azide in MeOH−H_2O medium (10:1, v/v) resulted in a 1D helical coordination polymer $[(CuL)Hg(N_3)_2]_n$ (**1**) and a trinuclear $[(CuL)_2Hg(N_3)_2]$ (**2**) complexes depending upon the molar ratios of "metalloligand" [CuL] and Hg(II) (Scheme 1). Complex **1** separated as a green solid when [CuL], mercuric nitrate monohydrate and sodium azide were mixed in 1:1:2 molar ratios. The diffraction quality needle shaped green single crystals of **1** were obtained on keeping the filtrate overnight at open atmosphere. A comparison of the powder XRD patterns (Figure S1, Supporting Information) of the green product with that of the simulated powder XRD pattern of the single crystal clearly shows that it is pure **1**. However, when the same components are mixed in 2:1:2 molar ratios, then a greenish brown crystalline compound was separated. The diffraction quality rectangular shaped greenish brown single crystals of **2** were obtained by the slow evaporation of the filtrate in open atmosphere. The greenish brown product is pure **2** as is evident from its powder XRD pattern (Figure S1). Complex $[(CuL)_2Cd(N_3)_2]$ (**3**) was synthesized by following a similar procedure to that of **2**, by using cadmium nitrate tetrahydrate instead of mercuric nitrate monohydrate. The brown microcrystalline product, which was isolated after mixing the components, is the pure **3** as its powder XRD pattern is identical to that of the simulated one (Figure S1). Interestingly, there is no change in the powder XRD pattern of the brown product even if the [CuL], cadmium nitrate tetrahydrate and sodium azide are mixed in 1:1:2 molar ratios. In both cases, the crystals which were isolated on slow evaporation of the filtrate were examined under the microscope and found to be of only one type; their elemental analyses and X-ray powder patterns correspond to the trinuclear compound **3**. Therefore, it may be concluded that depending upon the molar ratios of [CuL] and Hg(II) two different products **1** and **2** are formed. However, Cd(II) ion produces only compound **3**; change in the ratios of molar concentration of the [CuL] has no influence on the product formation.

IR and UV−Vis Spectra of the Complexes. All three complexes were initially characterized by the IR spectra. A strong and sharp band due to the azomethine υ(C═N) group of the Schiff base appears at 1619, 1614, and 1614 cm^{-1} for complexes **1**−**3** respectively (Figures S2−S4). The characteristic intense single peaks at 2045, 2036, and 2040 cm^{-1} for azido ligand were clearly detected in the IR spectra of **1**−**3** respectively.

The UV−vis spectra of the compounds in methanol and DSMO solutions and their solid state diffused reflectance spectra are shown in Figure 1, and the spectral parameters are given in Table 4. The complexes show a broad absorption band

Table 4. UV-Vis Spectral Parameters of the "Metalloligand", 1, 2, and 3

complex[a]	λ_{max}(nm) in MeOH	λ_{max}(nm) (ξ, M^{-1} cm^{-1}) in DMSO	λ_{max}(nm) in solid state
metalloligand	601, 358 and 270	601(136), 360 (8860) and 270 (19233)	596 and 382
1	596, 359 and 269	596 (230), 361(16394) and 274 (33673)	615 and 387
2	596, 360 and 273	597 (363), 360 (23150) and 272 (36739)	593 and 375
3	601, 358 and 273	597 (313), 361(19620) and 269(34978)	578 and 370

[a]All three complexes are sparingly soluble in methanol and therefore molar extinction coefficients are not given.

in the visible region at 596, 596, and 601 nm in methanol, 596, 597, and 597 nm in DMSO and 615, 593, and 578 nm in the solid state for **1**, **2**, and **3** respectively, attributed to d−d transitions of Cu(II) ions. The spectra of the complexes and of the mononuclear [CuL] precursor in solutions are very similar and suggest a square planar environment around Cu(II) in all of them. However, in the solid state spectra this band for **1** is 22 and 37 nm red-shifted compared to that of complexes **2** and **3** respectively. The shift of these absorption bands toward higher energies for **2** and **3** may be due to the weaker axial interaction around Cu(II) in **2** with respect to **1** and to the absence of any axial interaction[31,58] around Cu(II) in **3**. Therefore, it may be concluded that the solid state identity of the complexes is lost in solution. Besides this band, an absorption band in the range 359−387 nm, assignable to ligand-to-metal charge transfer transitions is observed for all three complexes.

Structure Description of the Complexes. The structure of **1** is shown in Figure 2 together with the atomic numbering scheme. Dimensions in the metal coordination sphere are given in Table 2. The asymmetric unit of this complex contains one "metalloligand" [CuL] (where H_2L = *N*,*N*′-bis(salicylidene)-1,3-propanediamine), one Hg(II) ion and two azide anions. Thus, a bimetallic unit of formula $[(CuL)Hg(N_3)_2]$ is formed.

dx.doi.org/10.1021/ic301773h | *Inorg. Chem.* 2012, 51, 12407−12418

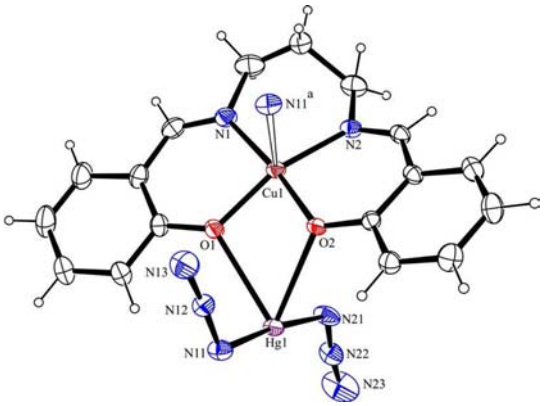

Figure 2. The structure of **1** with ellipsoids at 30% probability. The weak interactions are shown as an open bond.

The Cu(II) ion presents a penta-coordinated square pyramidal geometry where the basal plane is formed by the two imine N atoms and the two phenoxido O atoms of the Schiff base. The root mean squared (r.m.s.) deviation of the four basal atoms from the mean plane is 0.171 Å with the metal atom is 0.094(1) Å from this plane toward the axially coordinated nitrogen atom N(11)[a]. The axial Cu−N bond distance is significantly longer than the equatorial bonds (Table 2). The square pyramidal geometry around Cu(1) is slightly distorted as is indicated by the so-called Addison parameter (τ)[59] which is 0.144.

The mercury ion is bonded with two phenoxido oxygen atoms of the [CuL] and two nitrogen atoms of two different azido ligands. The Hg−O bond distances are significantly greater than that of the Hg−N bond distances (Table 2). The angle between the two coordinating nitrogen atoms around Hg atom [N(11)−Hg(1)−N(21) 173.17(17)°] is much wider than that between the two oxygen atoms [O(1)−Hg(1)−O(2) 58.85(9)°]. This causes a distortion of the tetrahedral geometry toward seesaw arrangement. Within the dimer Hg···Cu distance is 3.555(5) Å. Interestingly, the distances between the central nitrogen atoms of both the azido ligands (N12 and N22) and mercury atom [2.790(4) and 2.816(5) Å] are rather short. In the literature, similar distances have been described for the coordinate covalent bond in mercury(II) complexes. For instance a Hg−N distance of 2.764(6) Å has been observed in [2-(dimethylaminomethyl)phenyl]mercury(II) chloride,[60] 2.830(2) Å in catena-(μ_3-2,3-diphenyl-5,6-di(1H-tetrazol-5-yl)pyrazine)-diaqua-mercury (μ_3-2,3-diphenyl-5,6-di(1H-tetrazol-5-yl)pyrazine)-diaqua-mercury[61] and 2.897(2) Å in 2-chloromercuro-1-[(4-methoxyphenylimino)methyl]ferrocene.[62] These distances are significantly shorter than the sum of van der Waals radii of Hg (2.04 Å)[63] and N (1.55 Å),[64] however are longer than the sum of their covalent radii (2.03 Å).[65]

Among the two azido ligands, the N atom (N11) of one coordinates to the axial position of the Cu atom of another dinuclear unit (symmetry = x, 1/2 − y, 1/2 + z) in $\mu_{-1,1}$ bridging mode to form a 1D helical coordination polymer. In the crystal both right (M-helix) and left (P-helix) handed helical chains of this compound (Figure 3) are present in equal numbers. Hence there is no overall chirality and the complex crystallized in achiral space group ($P2_1/c$).

The structure of **2** is shown in Figure 4 together with the atomic numbering scheme. Dimensions in the metal coordination sphere are given in Table 2. The complex consists of a centrosymmetric trinuclear structure of formula $[(CuL)_2Hg(N_3)_2]$ with the three metal atoms in linear disposition. The

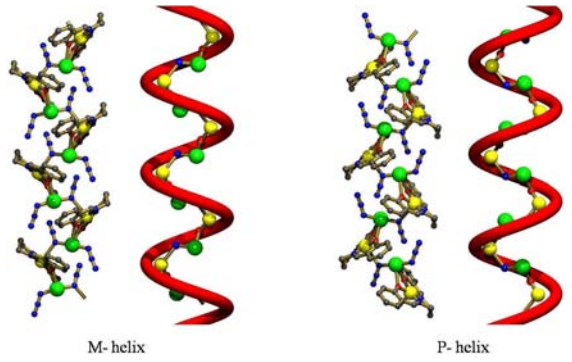

Figure 3. The 1D helical coordination polymer of **1** (green Hg, yellow Cu, blue N, red O). H-atoms have been removed for clarity.

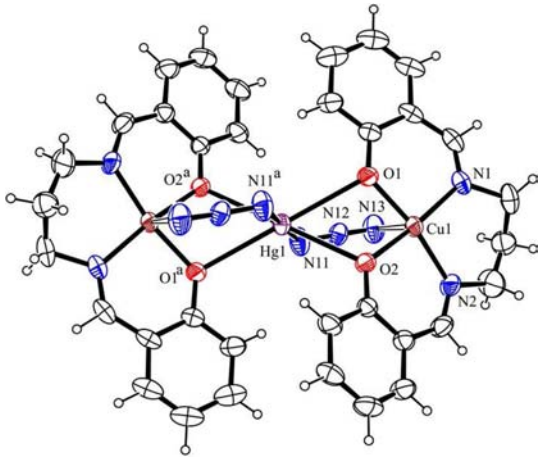

Figure 4. The structure of **2** with ellipsoids at 30% probability. The weak interactions are shown as an open bond.

two terminal Cu(II) ions possess a penta-coordinate, distorted square pyramidal coordination sphere. The basal plane in the copper ion is constituted by the two oxygen atoms and two nitrogen atoms from the Schiff base. The azido ligands which are bonded to central Hg atom, coordinate weakly *via* $\mu_{-1,3}$ bridging mode to the axial position of the terminal Cu(II) at distances Cu(1)−N(13) 2.855(6) Å to complete the penta-coordination geometry. The Addison parameter (τ) for Cu(1) is 0.024. The r.m.s. deviation of the four basal coordinating atoms from the mean plane passing through them is 0.115 Å. The metal atom is 0.002(1) Å from this plane toward the axially coordinating nitrogen atom N(13).

The mercury atom Hg(1) which sits on the crystallographic inversion center has a six coordinate compressed octahedral environment being bonded to the four oxygen atoms of the two different "metalloligands" at distances 2.762(4) and 2.687(4) Å in the basal plane. The two *trans* axial positions are occupied by the other terminal nitrogen atoms [N(11) and N(11)[a]] of the azido ligand at distance of 2.079(6) Å. The distance between the central nitrogen atom of azide ions and mercury atom is 2.823(4) Å. All the *trans* angles are ideal (180°) as the molecule possesses a center of inversion, but the *cis* angles [54.69(10)−125.31(10)°] deviate considerably from the ideal value (90°). The Hg···Cu distance is 3.708(2) Å.

The structure of **3** is shown in Figure 5 together with the atomic numbering scheme. Dimensions in the metal coordination sphere are given in Table 3. The complex consists of an bent trinuclear neutral unit of formula $[(CuL)_2Cd(N_3)_2]$. The

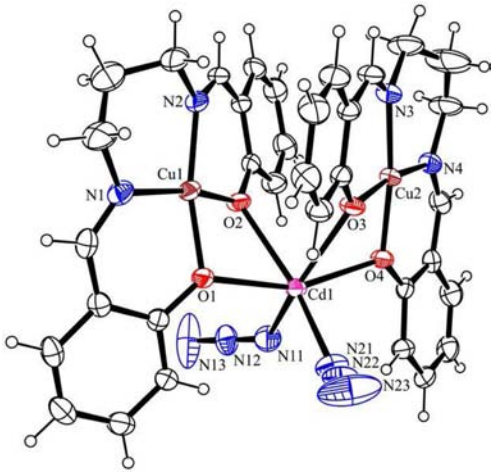

Figure 5. The structure of **3** with ellipsoids at 30% probability.

copper atoms are four coordinate with a distorted square planar environment being bonded to two oxygen atoms and two nitrogen atoms of the Schiff-base ligand. Unlike complex **2**, there are no axial interactions [Cu(1)···N(13) 5.333 Å and Cu(2)···N(21) 4.759 Å] between terminal Cu atoms and nitrogen atoms of azido ligands. The four donor atoms show r.m.s. deviations of 0.205 and 0.052 Å for Cu(1) and Cu(2) respectively with the copper atoms at 0.005(1) and 0.002(1) Å from their mean plane. The *trans* angles around Cu(1) and Cu(2) (Table 3) indicate that the geometry of Cu(1) is more distorted than that of Cu(2) from the ideal square planar geometry. The greater tetrahedral distortion around Cu(1) is also apparent in the dihedral angles between the two N−Cu−O planes, which are 16.99 and 4.29° for Cu(1) and Cu(2) respectively.

The cadmium ion has a six-coordinate distorted octahedral environment being coordinated to four oxygen atoms from the two different "metalloligand" and two terminal nitrogen atoms of two *cis* azido ligands. Both the *cis* [62.78(11)−101.70(14)°] and *trans* [151.50(14)−158.23(11)°] angles indicate considerable distortions from ideal octahedral geometry. The two Cd···Cu distances are 3.331(1) and 3.347(1) Å, while the Cu···Cu separation is 4.787 Å. Unlike complexes **1** and **2** the Cd atom is far from the central nitrogen atom of azide with a distance of 3.100(6) and 3.101(5) Å.

A CSD search for heterometallic Cu(II)−Hg(II) complexes containing a symmetrical tetradentate salen type Schiff base ligand reveals that complex **1** of the present work is the first report of a 1D helical coordination polymer of Cu(II)−Hg(II) system, although three discrete dinuclear [Cu(II)−Hg(II)] complexes (two with Cl^- and one with Br^-) are reported.[66−68] Complex **2** is only the second example of linear trinuclear $Cu(II)_2$-Hg(II) complexes; the other one is formed through a μ_2-thiocyanato-N,S bridge.[69] There are quite a few $Cu(II)_2$-Cd(II) complexes with both linear and bent structures.[7,32]

EPR Spectra of the Complexes. We have calculated the exchange parameter (J), Cu−Cu inter nuclear distance (r) and angle (ξ) between principal Z direction of the binuclear complex and Cu−Cu vector which are useful in getting information about the basic structure of these complexes. The EPR parameters for copper(II) ions in **1**−**3** have been precisely determined from the calculated spectra, which were obtained with the Bruker SIMFONIA program based on perturbation theory.[70] The theoretical EPR signals for mononuclear complexes ($S = 1/2$) in the axial field were calculated using the Spin Hamiltonian

$$\mathcal{H} = g_{\|}\beta H_z S_z + g_{\perp}\beta(H_x S_x + H_y S_y) + A_{\|}^{Cu} I_z S_z + A_{\perp}^{Cu}(I_x S_x + I_y S_y)$$

where H is the applied field, β is the Bohr magneton, S_x, S_y, S_z are the components of spin along three mutually perpendicular crystalline axes x, y and z, S is the total spin of the electron, and g is the spectroscopic factor. For binuclear complexes $S = 1$ and they were calculated using the spin Hamiltonian

$$\mathcal{H} = \beta g H S + D[S_z^2 - 1/3\{S(S+1)\}] + E(S_x^2 - S_y^2)$$

where D and E are second order crystal field terms with axial and rhombic−structure parameters. The spin Hamiltonian parameters obtained from the simulation of binuclear and mononuclear complexes are given in Table 5. It can be seen that there is a close agreement between the experimental and theoretical spectra (simulated spectra) thereby suggesting overall goodness of fit.

Table 5. EPR Parameters of the Complexes and Other Reported Copper(II) Mononuclear (M) and Binuclear (B) Complexes with Different Ligands[a]

matrix	$g_{\|}$	$g_{\perp}$	g_{iso}	$A_{\|}$(G)	$A_{\perp}$(G)	A_{iso}(G)	D (cm^{-1})	J (cm^{-1})	r (Å)	ref
$[Cu(NH_3)_4]^{2+}$ (M)	2.2160	2.0340	2.0947	160						73
$[Cu(NH_3)_4][PtCl_4]$ (M)	2.2170	2.0510	2.1063	211	28	89				74
$[Cu(1\text{- AMUH})_2]Cl_2$ (M)	2.2400	2.0600	2.1200	218	25	89				75
$[Cu(II)1\text{-PhAB}^{i}UH)en]_2(H_2O)_2(Cl)_2$ (B)	2.1640	2.0525	2.0900	100			0.0493	+55	3.99	76
$[Cu(II)1\text{-PhAB}^{i}UH)tn]_2(H_2O)_2(Cl)_2$ (B)	2.1730	2.0490	2.0903	100			0.0505	+50	3.98	77
$[Cu(1\text{-PhABUH})en(H_2O)]Cl_2$ (B)	2.1200	2.0530	2.0753	90			0.0525	+57	4.00	77
$Cu_3(BTC)_2$	2.3690	2.0600	2.1630				0.320			79
$(\mathbf{1})_1$[c]	2.2450	2.0540	2.1177	180						[b]
$(\mathbf{2})_1$	2.2460	2.0550	2.1187	178						[b]
$(\mathbf{3})_1$	2.2410	2.0540	2.1163	180						[b]
$(\mathbf{3})_2$	2.1650	2.0640	2.0977	75			0.0320	+210	4.50	[b]

[a] $PhAB^{n}UH$ = phenylamidino-*O*-*n*-butylurea, PhAMUH = phenylamidino-*O*-methylurea, $PhAB^{i}UH$ = phenyamidino-*O*-i-butylurea, AMUH = amidino-*O*-methylurea; en = 1,2- diaminoethane, tn = 1,3-diaminopropane, H_2L = *N*,*N*′-bis(salicylidene)-1,3-propanediamine; and BTC = benzene 1,3,5-tricarboxylate. Error in g is ±0.0001, in A is ±2 G and in D is ±5 G. [b] Present work. [c] 1 for mononuclear species and 2 for dinuclear species. Error in g is ±0.0001, in A is ±2 G and in D is ±5 G.

dx.doi.org/10.1021/ic301773h | *Inorg. Chem.* 2012, 51, 12407−12418

Room temperature EPR spectra of **1**−**3** in polycrystalline form consist of a weak shoulder at *g* ca. 2.2 and an intense signal at *g* ca. 2.06 having a typical derivative line shape (not shown in figure). These EPR features are characteristic of mononuclear Cu(II) complexes in polycrystalline samples with random orientation of microcrystallites. In order to reduce the broadening of the EPR signals caused by spin−spin interaction in solids and to resolve the hyperfine interaction, the EPR spectra of these heterometallic complexes in methanol and DMSO solutions were recorded at 100 K. The EPR spectra of magnetically diluted heteronuclear complexes **1** and **2** (Figure 6) showed an axially symmetric EPR spectrum consisting of the

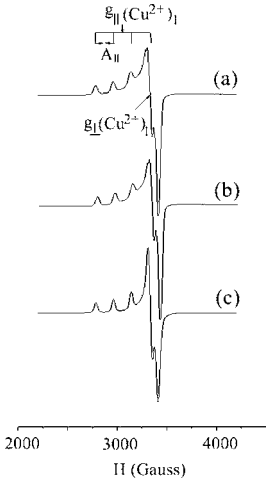

Figure 6. EPR spectra of complexes in DMSO at 100 K (a) for **1** (b) for **2**. (c) Simulated EPR spectrum using axial symmetry for mononuclear complex (S = 1/2).

parallel components ($g_{\|}$ = 2.245) and an intense perpendicular component ($g_{\perp}$ = 2.054). The observation of quartet hyperfine structure on the parallel component is due to interaction of unpaired electron of copper(II) with[63,65] Cu having nuclear spin I = 3/2.

The EPR spectrum of **3** in DMSO consisted of superposition of two spectra that could be deconvoluted into two axially symmetric spectra; the first one due to mononuclear complex as observed in **1** and **2**, while the second one was assigned to binuclear complex. The EPR spectra of binuclear complex consisted of an intense doublet (g ca. 2.05) due to fine-structure transitions ($\Delta M_s = \pm 1$) having zero-field splitting (ZFS) of 0.0320 cm^{-1} and a weak half-field signal ($\Delta M_s = \pm 2$) at g ca. 4.2 corresponding to forbidden transition suggesting the formation of binuclear copper complex. The presence of well resolved seven line hyperfine structure on the forbidden transition ($\Delta M_s = \pm 2$) with hyperfine coupling nearly half (A = 90 G) compared to that observed on the parallel component for the corresponding mononuclear complex (A = 178 G) further confirmed the formation of the binuclear complex. This is shown in Figure 7. The average distance (r) between the two unpaired electrons in binuclear complex was estimated by using $D = 3g^2\beta^2/2r^3 = 1.39 \times 10^4\ (g/r^3)$ where D is zero field splitting measured in Gauss and r in angstroms[71] (Table 5). The estimated average distance was 4.50 Å lower than 4.787 Å observed by X-ray crystallography. We have evaluated the angle ξ (41°) for **3** using the equation $g_z^2 = g_{\|}^2 \cos^2(\xi) + g_{\perp} \sin^2(\xi)$,[72] where $g_{\|}$ (2.241) and $g_{\perp}$ (2.054) represent g values for the mononuclear complex, ξ is the angle between the Cu−Cu

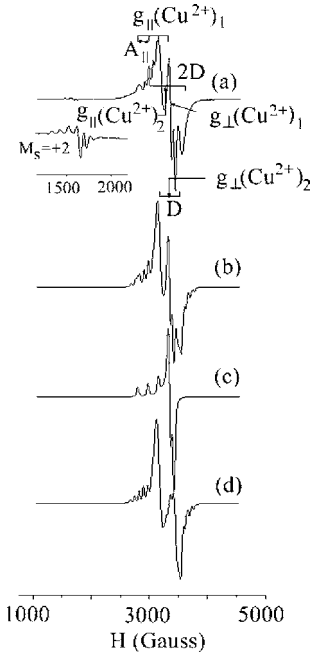

Figure 7. (a) EPR spectrum of complex **3** in DMSO at 100 K. (b) Simulated EPR spectrum using mononuclear (S = 1/2) and binuclear (S = 1) complexes in the weight ratio 1:1.25. The EPR parameters used for simulation of mononuclear and binuclear complexes are listed in Table 5. (c) Simulated EPR spectrum for mononuclear complex (S = 1/2) (d) simulated EPR spectrum for binuclear complex (S = 1). The inset showing forbidden $\Delta M_s = \pm 2$ transition (half field signal) characteristic of binuclear complex.

direction and the parallel direction and $g_{\|}$ is replaced by g_z^2(2.1650) as $g_{\|}$ and Cu−Cu direction for binuclear complex do not coincide.

We have recorded the EPR spectra of **3** in the temperature range 100−220 K. The population of the triplet state is governed by Boltzmann distribution and the Curie law following eq $3/T\ \exp(-J/\kappa T)$ where k is the Boltzmann constant and J is exchange parameter. From this equation, the isotropic exchange interaction constant J was calculated by following the temperature dependence of the peak to peak intensity (I) of the allowed EPR transitions, $\Delta M_s = \pm 1$ for these complexes which is shown in Figure 8.

EPR spectra of copper(II) having perfect square planar geometry of four equivalent nitrogen donor atoms around the copper(II) ion, viz CuN_4^{2-} has been reported[73−78] in a number of mononuclear complexes. The reported spectrum in their study showed a well resolved nine component super hyperfine structure (SHFS) suggesting nearly square planar coordination of four equivalent nitrogen donor atoms around the copper ion. It may be noted from the crystal structure that **1**−**3** exhibits distorted square planar geometry around Cu(II) ions consisting of two nitrogen atoms and two oxygen atoms (differing in bond lengths) yielding $[CuN_2O_2]$ building blocks. In addition to regular 4-fold coordination $[CuN_2O_2]$, **1** and **2** exhibit weak apical coordination of nitrogen atoms from the azido ligand. The absence of superhyperfine structure in present EPR studies may be because of the presence of nonequivalent nitrogen atoms in the coordination polyhedral around Cu(II) ions. The trend in the g value ($g_{\|} > g_{\perp} > 2.00$) suggested that the unpaired electron in the copper(II) ion is in the $d_{x^2-y^2}$ orbital.

Electrospray Ionization Mass Spectrometry of the Complexes. In order to investigate the species present in

dx.doi.org/10.1021/ic301773h | *Inorg. Chem.* 2012, 51, 12407−12418

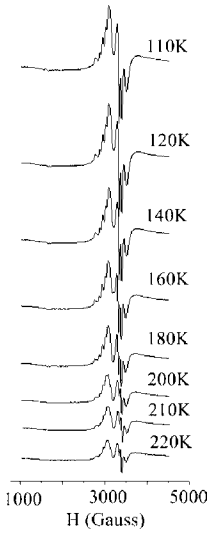

Figure 8. Temperature dependence of the EPR spectra of **3** in DMSO in the temperature range 110−220 K.

solution, the electrospray ionization mass spectra (ESI-MS positive) of **1**−**3** were also recorded in methanolic solution (Figures S5−S7). The spectra of the three complexes show a similar pattern with the base peak at m/z = 708.8 (100%) which can be assigned to the cationic species $[(CuL)_2Na]^+$. The peaks due to the $[(CuL)_2H]^+$ species are observed in all complexes at m/z = 686.9. The peaks at m/z = 343.9 and 365.9 indicate the formation of the $[(CuL)H]^+$ and $[(CuL)Na]^+$ species in solution. For all three complexes the appearance of another peak at m/z = 1053.8 may be attributed to the presence of $[(CuL)_3Na]^+$ species. The dominance of the Na-containing species is likely because the Na^+ ion which is released from the matrix forms more a stable complex than Hg^{2+} or Cd^{2+} with [CuL]. However, if we consider only the proton containing cationic species it can be found that the intensity ratio of binuclear/mononuclear species in complex **3** is significantly higher than those in complexes **1** and **2**, corroborating the observed EPR signal for the binuclear species only in **3**.

Theoretical Study and CSD Analysis. The structures of heterometallic complexes **1** and **2** have been described above. One question raised is the possibility of an additional interaction between the Hg atom and the central nitrogen atom of azido ligands in both complexes and even the interaction between the third nitrogen atom N(13) of the azido ligands and Cu atom in **2**. Compound **1** is a 1D helical coordination polymer where one azido ligand is monocoordinated and the other one is coordinated simultaneously to Hg(II) and Cu(II) metal ions through $\mu_{-1,1}$ azido bridging facilitating the formation of a 1D helical coordination polymer. Compound **2** is a discrete trinuclear complex where both azido ligands are only coordinated to Hg(II). Interestingly, in **2** a weak interaction between the ending nitrogen atom of the azido ligand and the Cu(II) metal ion is established (Figure 9). The Cu(1)−N(13) distance in compound **2** is 2.854(6) Å, which is only 0.2 Å longer than the Cu(1)−N(11)[a] polymeric bond in **1** (2.635(5) Å). This additional interaction contributes to the smaller Hg(1)−N(11)−N(12) angle observed in **2**.

Curiously, the bond distances between the Hg atoms and the central nitrogen atom of the azido ligands are 2.790(4) and 2.816(5) Å in **1** and 2.823(4) Å in **2**. These bond distances are significantly less than the sum of van der Waals radii of mercury (2.04 Å) and nitrogen (1.55 Å) and considerably longer than the sum of their covalent radii (2.03 Å). We have studied theoretically if there is an additional interaction between the central nitrogen atom of the azido ligand and the mercury. First, we have examined the CSD database in order to find similar complexes. We have restricted the search to Hg(II) complexes and azido ligands that are not coordinated using both ending nitrogen atoms of the azide. We have found a very small number of hits (nine). Only in one structure the distance between the central nitrogen atom of the azido ligand and the Hg is as short as the compounds reported herein. This structure is shown in Figure 10 and corresponds to EJOQEA. The Hg(2)−N(14) distance is 2.820(7) Å and the Hg(2)−N(13)−N(14) angle is 119.2°.

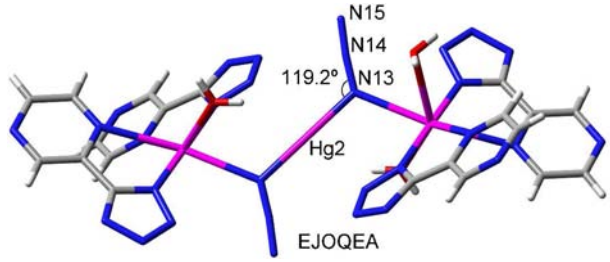

Figure 10. Representation of the EJOQEA structure.

The distances and angles of all structures are summarized in Table 6, where we have included the data of compounds **1** and **2** for comparison purposes. It can be observed that the distances vary from 2.791 Å (compound **1**) to 3.033 Å (MHGAZD) and the angles from 113.76° (FODKIT) to 127.18° (FMHGAZ). Therefore, it is clear that the preference angle for this ligand is around 120°.

This part of the theoretical study has been performed using the RI-MP2/aug-cc-pVDZ method, since the size of the system allows the use of high level calculations. We have first used a small model in order to study the preference of the Hg−N−N angle, namely, azido-methyl-mercury(II). It can be observed

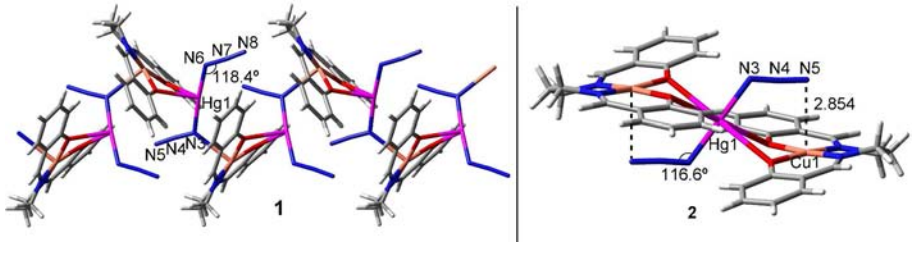

Figure 9. Heteronuclear complexes **1** and **2**.

dx.doi.org/10.1021/ic301773h | *Inorg. Chem.* 2012, 51, 12407−12418

Table 6. Distances and Angles of 1, 2 and the Structures Found in the CSD

structure	Hg−N(2) (Å)	Hg−N(1)−N(2) (deg)	ref
1	2.791/2.815	114.98/118.37	present work
2	2.824	116.65	present work
AQAMOV	2.860	119.93	34
AQAMUB	2.883	116.05	34
EJOQEA	2.820	119.18	33
FMHGAZ	2.907	127.18	35
FODKIT	2.882	113.76	36
MHGAZD	3.033	123.25	78
MHGAZD01	2.893	117.91	37
PEXHEG	2.900	121.01	38
TUWREJ	2.943/3.001	120.28/117.00	39

that the optimized geometry is very similar to the crystallographic one (Figure 11). The Hg−N(1)−N(2) angle is close to

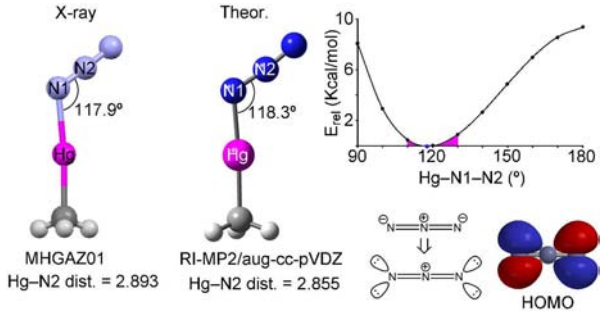

Figure 11. Left: X-ray and optimized geometries of azido-methyl-mercury(II). Top right: energetic profile varying the Hg−N(1)−N(2) angle. Bottom right: HOMO representation of the azide ion and the main resonance form.

118° and the Hg−N(2) distance is 2.855 Å, which agrees with the values found in compounds **1** and **2**. An additional interaction between Hg and N(2) is not expected taking into account the major resonance form of the azide anion, where the central nitrogen atom is not electron rich. The directionality of the azido ligand when coordinated to the nondirectional d^{10} Hg(II) metal is due to the electronic nature of the azide, where the electron pairs form an angle of approximately 120° with the N═N bond, as is confirmed by the HOMO representation shown in Figure 11. The energetic profile shown in Figure 11 has been computed varying the Hg−N(1)−N(2) angle. It clearly shows that angles ranging from 110 to 120 degrees are favored for this type of complex, in agreement with the values gathered in Table 6. For angles lesser than 110° the energy rises rapidly and for angles greater than 130 the energy rises more gradually.

We have also computed the distribution of critical points in complexes **1** and **2** in order to confirm the absence of interaction between the Hg and the central nitrogen atom of the azido ligands and to confirm the ancillary Cu(1)−N(13) interaction in compound **2**. Since compound **1** is polymeric, we have used a monomer to perform the calculations. In this case we have used DFT calculations (BP86-D) to perform the AIM analysis in order to keep the computation approachable. The representation of the critical points and bond paths connecting the bond critical points with the nuclear positions is shown in Figure 12. In compound **2**, it can be observed the presence of a critical point connecting the N(13) with the copper atom that corroborates this ancillary interaction. In addition, the presence of a critical point connecting the Hg with the central nitrogen atom of the azido ligand in both compounds is not observed, which likely means the absence of any interaction between both atoms.

Finally, we have analyzed theoretically and using the CSD the different molecular shapes observed experimentally for complexes **2** and **3**, as it has been described in the Structure Description of the Complexes (*vide supra*). One important difference observed in both complexes is the M(II)−N11−N12 (M = Hg, Cd) angle. That is, in compound **2** the value for the Hg(1)−N(11)−N(12) angle is 116.6°, while in compound **3** the values are 133.6° for Cd(1)−N(11)−N(12) and 133.9° for Cd(1)−N(21)−N(22). In order to know if there is a preference for small angles in Hg(II) complexes compared to Cd(II) complexes, we have analyzed the CSD. In Figure 13 we

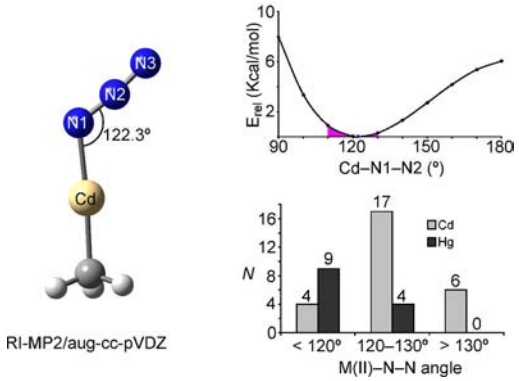

Figure 13. Left: Optimized geometry of azido-methyl-cadmium(II). Top right: energetic profile varying the Cd−N(1)−N(2) angle. Bottom right: Histogram plot obtained for the M(II)−N−N angle in Hg(II) and Cd(II) complexes with terminal azido ligand.

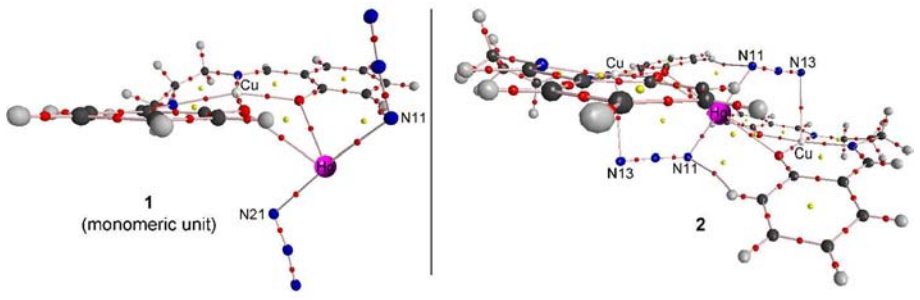

Figure 12. Distribution of critical points (CPs) in compounds **1** and **2** and the bond paths connecting bond CPs. The bond and ring CPs are represented by red and yellow spheres, respectively.

dx.doi.org/10.1021/ic301773h | *Inorg. Chem.* 2012, 51, 12407−12418

show the histogram plots for this angle obtained from the CSD search and including the complexes reported in this work, as well. Interestingly, it can be clearly observed that Hg(II) complexes prefer angles smaller than 120°, in agreement with the theoretical calculations that give an ideal angle of 118° (Figure 11). In contrast Cd(II) complexes have a preference for angles greater than 120 deg. In fact, there are 17 structures with angles greater than 120° for Cd(II) and only 4 for Hg(II). Furthermore, there are six structures with angles greater that 130° for Cd(II) and none for Hg(II). Theoretically the ideal angle is 122.1° for cadmium, and the computed energy profile indicates that the relative energy does not vary significantly between 120 and 130° (only 0.3 kcal/mol), in sharp agreement with the histogram plot. It is worth mentioning that the energy profile computed for Hg (Figure 11) is significantly different than Cd around the minimum; see the highlighted region of the energy profile plot in Figures 11 and 13. It is clear that the Hg(II) complexes are able to reduce the angle to 110° without energy cost, and it is more difficult to augment the angle to 130° and the opposite is found for Cd complexes, also in agreement with the histogram plot. Combining the theoretical and CSD studies, we demonstrate that Hg(II)-azide complexes prefer angles from 110 to 120° that favor the formation of linear trinuclear complexes and allow the azido ligands to link the central mercury atom with the terminal copper atoms *via* $\mu_{1,3}$ bridges. In contrast the Cd(II)-azide complexes prefer angles around 130° that are too large to make possible the formation of the $\mu_{1,3}$ bridge, and this likely provokes the bent conformation observed in complex **3**. In this complex the azido ligand establishes a multitude of hydrogen bonds with neighboring molecules in the solid state that further stabilize this conformation.

CONCLUSIONS

In conclusion, the reaction of a "metalloligand" [CuL] with Hg(II) and Cd(II) resulted in two heterometallic copper(II)−mercury(II) and one copper(II)−cadmium(II) complexes. Two azido coligands are present in all complexes that exhibit different coordination behaviors. While complex **1** is a 1D helical coordination polymer constructed by joining the dinuclear units through single $\mu_{1,1}$ azido bridges, complex **2** is a linear trinuclear entity, in which two terminal "metalloligands" [CuL] are coordinated to a central Hg(II), which is linked additionally to the terminal copper atoms *via* $\mu_{1,3}$ azido bridges. In complex **3**, two mutually *cis* azido ligands are terminally coordinated to the central Cd(II) and consequently the trinuclear structure becomes bent. An interesting feature of compounds **1** and **2** is that the bond distance between the Hg atom and the central nitrogen atom of the azido ligands is significantly less than the sum of van der Waals radii and than reported Hg−N bond distances of some Hg(II) complexes. However, a theoretical *ab initio* study concludes that there is not any interaction between the central nitrogen atom of the azido ligand and the mercury, which is in agreement with the "atoms-in-molecules" analysis of the X-ray geometries. Finally, the different molecular shapes observed for trinuclear complexes **2** and **3** have been also studied and explained by analyzing the M(II)−N−N (M = Hg, Cd) angle preference from both theoretical and CSD experimental data. Several experimental observations including EPR and electrospray ionization mass spectrometry indicate that the observed solid state structures of all the complexes are lost in the solutions where for **1** and **2** the mononuclear complex [CuL] and for **3** both mononuclear and binuclear complexes $[CuL]_2$ dominate.

ASSOCIATED CONTENT

Supporting Information

Powder X-ray pattern, IR spectra and electrospray ionization mass spectra (ESI-MS positive) of complexes **1**−**3** are given in Figures S1−S7. Crystallographic data is also given in CIF format. These data can be obtained free of charge via the Internet at http://pubs.acs.org.

AUTHOR INFORMATION

Corresponding Author

*E-mail: toni.frontera@uib.es (A.F.); ghosh_59@yahoo.com (A.G.).

Notes

The authors declare no competing financial interest.

ACKNOWLEDGMENTS

L.K.D. is thankful to CSIR, India, for awarding Junior Research Fellowship [Sanction No. 09/028 (0805)/2010-EMR-I]. Crystallography was performed at the DST-FIST; India funded Single Crystal Diffractometer Facility at the Department of Chemistry, University of Calcutta. We thank CONSOLIDER−Ingenio 2010 (projects CSD2010-0065) and the MICINN of Spain (Projects CTQ2011-27512, FEDER funds) for financial support. We thank the Direcció General de Recerca, Desenvolupament Tecnològic i Innovació del Govern Balear (Accions Especials, 2011) for financial support. We thank the CESCA for computational facilities.

REFERENCES

(1) Vaz, M. G. F.; Pinheiro, L. M. M.; Stumpf, H. O.; Alcântara, A. F. C.; Golhen, S.; Ouahab, L.; Cador, O.; Mathonière, C.; Kahn, O. *Chem.—Eur. J.* **1999**, *5*, 1486−1495.
(2) Gheorghe, R.; Cucos, P.; Andruh, M.; Costes, J. -P.; Donnadieu, B.; Shova, S. *Chem.—Eur. J.* **2006**, *12*, 187−203.
(3) Dincá, M.; Long, J. R. *J. Am. Chem. Soc.* **2005**, *127*, 9376−9377.
(4) Berenguer, J. R.; Lalinde, E. M.; Moreno, T. *Coord. Chem. Rev.* **2010**, *254*, 832−841.
(5) Coronado, E.; Galán-Mascarós, J. R.; Gómez-García, C. J.; Laukhin, V. *Nature* **2000**, *408*, 447−449.
(6) Das, L. K.; Drew, M. G. B.; Ghosh, A. *Inorg. Chim. Acta* **2013**, *394*, 247−254.
(7) Biswas, S.; Ghosh, A. *Polyhedron* **2011**, *30*, 676−681.
(8) Biswas, S.; Ghosh, A. *Indian J. Chem. Sec. A* **2011**, *50A*, 1356−1362.
(9) Biswas, S.; Naiya, S.; Gómez-García, C. J.; Ghosh, A. *Dalton Trans.* **2012**, *41*, 462−473.
(10) Seth, P.; Das, L. K.; Drew, M. G. B.; Ghosh, A. *Eur. J. Inorg. Chem.* **2012**, 2232−2242.
(11) Biswas, S.; Saha, R.; Ghosh, A. *Organometallics* **2012**, *31*, 3844−3850.
(12) Novitchi, G.; Shova, S.; Caneschi, A.; Costes, J. -P.; Gdaniec, M.; Stanica, N. *Dalton Trans.* **2004**, 1194−1200.
(13) Ulku, D.; Tatar, L.; Atakol, O.; Durmus, S. *Acta Crystallogr.* **1999**, *C55*, 1652−1654.
(14) Fukuhara, C.; Tsuneyoshi, K.; Matsumoto, N.; Kida, S.; Mikuriya, M.; Mori, M. *J. Chem. Soc., Dalton Trans.* **1990**, 3473−3479.
(15) Ercan, F.; Ulku, D.; Atakol, O.; Dincer, F. N. *Acta Crystallogr.* **1998**, *C54*, 1787−1790.
(16) Atakol, O.; Durmus, S.; Durmus, Z.; Arici, C.; Cicek, B. *Synth. React. Inorg. Met.-Org. Chem.* **2001**, *31*, 1689−1692.
(17) Ray, A.; Rosair, G. M.; Rajeev, R.; Sunoj, R. B.; Rentschler, E.; Mitra, S. *Dalton Trans.* **2009**, 9510−9519.

(18) Epstein, J. M.; Figgis, B. N.; White, A. H.; Willis, A. C. *J. Chem. Soc., Dalton Trans.* **1974**, 1954−1961.
(19) Adhikary, C.; Koner, S. *Coord. Chem. Rev.* **2010**, *254*, 2933−2958.
(20) Naiya, S.; Biswas, C.; Drew, M. G. B.; Gómez-García, C. J.; Clemente-Juan, J. M.; Ghosh, A. *Inorg. Chem.* **2010**, *49*, 6616−6627.
(21) Chaudhuri, P.; Weyhermtiller, T.; Bill, E.; Wieghardt, K. *Inorg. Chim. Acta* **1996**, *252*, 195−202.
(22) Ribas, J.; Escuer, A.; Monfort, M.; Vicente, R.; Cortěs, R.; Lezama, L.; Rojo, T. *Coord. Chem. Rev.* **1999**, *193*, 1027−1068.
(23) Dalai, S.; Mukherjee, P. S.; Mallah, T.; Drew, M. G. B.; Ray Chaudhuri, N. *Inorg. Chem. Commun.* **2002**, *5*, 472−474.
(24) Mukherjee, S.; Gole, B.; Song, Y.; Mukherjee, P. S. *Inorg. Chem.* **2011**, *50*, 3621−3631.
(25) Mukherjee, P. S.; Maji, T. K.; Escuer, A.; Vicente, R.; Ribas, J.; Rosair, G.; Mautner, F. A.; Ray Chaudhuri, N. *Eur. J. Inorg. Chem.* **2002**, 943−949.
(26) Mukherjee, S.; Patil, Y. P.; Mukherjee, P. S. *Dalton Trans.* **2012**, *41*, 54−64.
(27) Goher, M. A. S.; Mak, T. C. W. *Inorg. Chim. Acta* **1985**, *99*, 223−229.
(28) Escuer, A.; Aromí, G. *Eur. J. Inorg. Chem.* **2006**, 4721−4736.
(29) Papaefstathiou, G. S.; Perlepes, S. P.; Escuer, A.; Vicente, R.; Font-Bardia, M.; Solans, X. *Angew. Chem., Int. Ed.* **2001**, *40*, 884−886.
(30) Papaefstathiou, G. S.; Escuer, A.; Vicente, R.; Font-Bardia, M.; Solans, X.; Perlepes, S. P. *Chem. Commun.* **2001**, 2414−2415.
(31) Das, L. K.; Park, S. -W.; Cho, S. J.; Ghosh, A. *Dalton Trans.* **2012**, *41*, 11009−11017.
(32) Das, L. K.; Biswas, A.; Frontera, A.; Ghosh, A. *Polyhedron* **2012**, DOI: 10.1016/j.poly.2012.04.029.
(33) Yang, E. -C.; Feng, Y.; Liu, Z. -Y.; Liu, T. -Y.; Zhao, X. -J. *CrystEngComm* **2011**, *13*, 230−242.
(34) Klapötke, T. M.; Krumm, B.; Moll, R. *Z. Anorg. Allg. Chem.* **2011**, *637*, 507−514.
(35) Brauer, D. J.; Bijrger, H.; Pawelke, G. *J. Organomet. Chem.* **1978**, *160*, 389−401.
(36) Chand, B. G.; Ray, U. S.; Mostafa, G.; Cheng, J.; Lu, T. -H.; Sinha, C. *Inorg. Chim. Acta* **2005**, *358*, 1927−1933.
(37) Mueller, U. *Z. Naturforsch., B: Chem. Sci.* **1973**, *28*, 426−429.
(38) Atoub, N.; Mahmoudi, G.; Morsali, A. *Inorg. Chem. Commun.* **2007**, *10*, 166−169.
(39) Chattopadhyay, S.; Bhar, K.; Das, S.; Satapathi, S.; Fun, H. -K.; Mitra, P.; Ghosh, B. K. *Polyhedron* **2010**, *29*, 1667−1675.
(40) Bader, R. F. W. *Atoms in Molecules-A Quantum Theory*; University Press: Oxford, 1990.
(41) Drew, M. G. B.; Prasad, R. N.; Sharma, R. P. *Sect. C: Cryst. Struct. Commun.* **1985**, *41*, 1755−1758.
(42) *SAINT, version 6.02; SADABS, version 2.03*; Bruker AXS, Inc., Madison, WI, 2002.
(43) Sheldrick, G. M. *SHELXS 97, Program for Structure Solution*; University of Göttingen: Germany, 1997.
(44) Sheldrick, G. M. *SHELXL 97, Program for Crystal Structure Refinement*, University of Göttingen: Germany, 1997.
(45) Spek, A. L. *J. Appl. Crystallogr.* **2003**, *36*, 7−13.
(46) Farrugia, L. J. J. *Appl. Crystallogr.* **1999**, *32*, 837−838.
(47) Farrugia, L. J. J. *Appl. Crystallogr.* **1997**, *30*, 565.
(48) Ahlrichs, R.; Bär, M.; Hacer, M.; Horn, H.; Kömel, C. *Chem. Phys. Lett.* **1989**, *162*, 165−169.
(49) Feyereisen, M. W.; Fitzgerald, G.; Komornicki, A. *Chem. Phys. Lett.* **1993**, *208*, 359−363.
(50) Frontera, A.; Quiñonero, D.; Garau, C.; Ballester, P.; Costa, A.; Deyà, P. M. *J. Phys. Chem. A* **2005**, *109*, 4632−4637.
(51) Quiñonero, D.; Garau, C.; Frontera, A.; Ballester, P.; Costa, A.; Deyà, P. M. *J. Phys. Chem. A* **2006**, *110*, 5144−5148.
(52) Quiñonero, D.; Estarellas, C.; Frontera, A.; Deyà, P. M. *Chem. Phys. Lett.* **2011**, *508*, 144−148.
(53) Grimme, S. *J. Comput. Chem.* **2006**, *27*, 1787−99.
(54) Bader, R. F. W. *Chem. Rev.* **1991**, *91*, 893−928.
(55) Grabowski, S. J.; Pfitzner, A.; Zabel, M.; Dubis, A. T.; Palusiak, M. *J. Phys. Chem. B* **2004**, *108*, 1831−1837.
(56) Vila, A.; Mosquera, R. A. *J. Mol. Struct. (THEOCHEM)* **2001**, *546*, 63−72.
(57) Chopra, D.; Cameron, T. S.; Ferrara, J. D.; Guru Row, T. N. *J. Phys. Chem. A* **2006**, *110*, 10465−10477.
(58) Roy, S.; Mitra, P.; Patra, A. K. *Inorg. Chim. Acta* **2011**, *370*, 247−253.
(59) Addison, A. W.; Rao, T. N.; Reedijk, J.; Van Rijn, J.; Verschoor, G. C. *J. Chem. Soc., Dalton Trans.* **1984**, 1349−1356.
(60) Bumbu, O.; Silvestru, C.; Gimeno, M. C.; Laguna, A. *J. Organomet. Chem.* **2004**, *689*, 1172−1179.
(61) Tao, Y.; Li, J.-R.; Chang, Z.; Bu, X.-H. *Cryst. Growth Des* **2010**, *10*, 564−574.
(62) Huo, S. Q.; Wu, Y. J.; Zhu, Y.; Yang, L. *J. Organomet. Chem.* **1994**, *470*, 17−22.
(63) Batsanov, S. S. *J. Mol. Struct.* **2011**, *990*, 63−66.
(64) Bondi, A. *J. Phys. Chem.* **1964**, *68*, 441−451.
(65) Cordero, B.; Gómez, V.; Platero-Prats, A. E.; Revés, M.; Echeverría, J.; Cremades, E.; Barragán, F.; Alvarez, S. *Dalton Trans.* **2008**, 2832−2838.
(66) Atakol, O.; Arici, C.; Tahir, M. N.; Kenar, A.; Ulku, D. *Acta Crystallogr.* **1999**, *C55*, 1416−1418.
(67) Kaynak, F. B.; Ulku, D.; Atakol, O.; Durmus, S. *Acta Crystallogr.* **1999**, *C55*, 1784−1785.
(68) Colon, M. L.; Qian, S. Y.; Vanderveer, D.; Bu, X. R. *Inorg. Chim. Acta* **2004**, *357*, 83−88.
(69) Yildirim, L. T.; Kurtaran, R.; Namli, H.; Azaz, A. D.; Atakol, O. *Polyhedron* **2007**, *26*, 4187−4194.
(70) Weber, R. T. *WIN-EPR SIMFONIA Manual*; Bruker: Madison, WI, 1995.
(71) Eaton, S. S.; More, K. M.; Sawant, B. M.; Eaton, G. R. *J. Am. Chem. Soc.* **1983**, *105*, 6560−6561.
(72) Chikira, M.; Kon, H. *J. Chem. Soc., Dalton Trans.* **1979**, 245−249.
(73) Williamson, W. B.; Lunsford, J. H. *J. Phys. Chem.* **1976**, *80*, 2664−2671.
(74) Raynor, J. B.; Teil, B. *Z. Naturforsch.* **1969**, *241*, 775−788.
(75) Wasson, J. R.; Trapp, C. *J. Phys. Chem.* **1969**, *73*, 3763−3778.
(76) Pramodini, S. D.; Hemakumar, R. K. S.; Kadam, R. M. *Inorg. Chem.* **2006**, *45*, 2193−2198.
(77) Pramodini, S. D.; Mimoda, S. D.; Shantibala, N. D.; Hemakumar, R. K. S.; Manoj, M.; Kadam, R. M. *Inorg. Chem. Commun.* **2008**, *11*, 1441−1444.
(78) Jaideva, L. S.; Shantibala, N. D.; Pramodini, S. D.; Bembee, W. D.; Hemakumar, R. K. S.; Rajeswari, B.; Kadam., R. M. *Inorg. Chem. Commun.* **2010**, *13*, 365−368.
(79) Poppl, A.; Kunz, S.; Himsl, D.; Hurtmann, M. *J Phys. Chem. C* **2008**, *112*, 2678−2684.